Check for updates

AGU100 ADVANCING EARTH AND SPACE SCIENCE

Water Resources Research

RESEARCH ARTICLE
10.1029/2019WR025350

Key Points:
- Based on a novel seasonal mountain snow mask, mountains with seasonal snow account for 31% of global snow cover and 9% of land area
- Global data sets estimate more than 1,100 km^3 of snow storage in global mountains
- Compared to regional model estimates, global data sets may underestimate mountain snow storage by 1,500 km^3, a bias exceeding 50%

Supporting Information:
- Supporting Information S1

Correspondence to:
M. L. Wrzesien,
wrzesien@unc.edu

Citation:
Wrzesien, M. L., Pavelsky, T. M., Durand, M. T., Dozier, J., & Lundquist, J. D. (2019). Characterizing biases in mountain snow accumulation from global data sets. *Water Resources Research*, *55*, 9873–9891. https://doi.org/10.1029/2019WR025350

Received 11 APR 2019
Accepted 19 AUG 2019
Published online 27 NOV 2019

©2019. American Geophysical Union. All Rights Reserved.

Characterizing Biases in Mountain Snow Accumulation From Global Data Sets

Melissa L. Wrzesien[1], Tamlin M. Pavelsky[1], Michael T. Durand[2], Jeff Dozier[3], and Jessica D. Lundquist[4]

[1]Department of Geological Sciences, University of North Carolina at Chapel Hill, Chapel Hill, NC, USA, [2]School of Earth Sciences and Byrd Polar and Climate Research Center, Ohio State University, Columbus, OH, USA, [3]Bren School of Environmental Science and Management, University of California, Santa Barbara, CA, USA, [4]Civil and Environmental Engineering, University of Washington, Seattle, WA, USA

Abstract Mountain snow has a fundamental role in regional water budgets through its seasonal accumulation, storage, and melt. However, characterizing snow accumulation over large regions remains difficult because of limited observational networks and the inability of available satellite instruments to remotely sense snow depth or water equivalent in mountains. Models offer some ability to estimate snow water storage (SWS) on mountain range to continental scales. Here we compare four commonly used global data sets to understand whether there is a consensus regarding mountain SWS estimates among them. The data sets—European Centre for Medium-Range Weather Forecasts Reanalysis-Interim, Global Land Data Assimilation System, Modern-Era Retrospective Analysis for Research and Applications version 2, and Variable Infiltration Capacity—agree to within ±36% of the four–data set average for total global SWS. When mountain areas are extracted using a new seasonal mountain snow classification data set, the four data products have more agreement, where all are within ±21% of the seasonal SWS for mountain regions. However, when compared to high-resolution (9 km) simulations of SWS from the Weather Research and Forecasting (WRF) regional model, the four global products differ from WRF-estimated North American mountain snow accumulation by 40–66%, with a negative bias up to 651 km^3, comparable to the annual streamflow of the Mississippi River. If we extend the North America SWS bias to global mountains, the global data sets may miss as much as 1,500 km^3 of SWS, equivalent to 4% of the flow in all the world's rivers. The potential difference of SWS suggests more work must be done to characterize water resources in snow-dominated regions, particularly in mountains.

1. Introduction

Mountains play an integral role in the global water budget by acting as natural "water towers" (Viviroli et al., 2007), especially through the storage of seasonal snowfall. Not only do mountains disproportionately store more water as snow than nonmountain areas (Mudryk et al., 2015; Snauffer et al., 2016; Wrzesien et al., 2018), but mountain snowmelt has a critical role in driving river runoff, especially in semiarid regions such as in the western United States (Li et al., 2017). In the Northern Hemisphere, snow is the largest contributor to seasonal variation in water storage (Zhou et al., 2016). Snow is estimated to be a trillion-dollar resource (Sturm et al., 2017), highlighting its usefulness to humans and the critical importance of understanding current patterns and future projections of snow accumulation in mountainous regions.

Estimating snow accumulation on the mountain range scale remains the biggest challenge of snow hydrology (Bormann et al., 2018; Dozier et al., 2016). As Lettenmaier et al. (2015) note in their review of hydrologic remote sensing, mapping of snow cover from satellite was among the first applications of the technology to hydrologic science (Barnes & Bowley, 1968). Now, daily global snow cover products are available at 500-m spatial resolution (Hall et al., 2002), and advances in analysis enable mapping of snow albedo by estimating the snow grain size (Painter et al., 2009) and the darkening by light-absorbing particles like dust or soot (Painter et al., 2012). However, remotely sensing the rate at which snow falls (Skofronick-Jackson et al., 2013) or snow depth or snow water equivalent (SWE) has proved elusive (Nolin, 2010), especially in the mountains. Dozier et al. (2016) describe the strengths and weaknesses of five approaches to the problem. One promising approach is the measurement of snow depth with lidar altimetry, as implemented by NASA's Airborne Snow Observatory (Painter et al., 2016), but an airborne program cannot acquire the

global data needed to cover the world's mountains. Lettenmaier et al. (2015) conclude their review with the statement, "Among all areas of hydrologic remote sensing, snow (SWE in particular) is the one that is most in need of new strategic thinking from the hydrologic community." Until that approach bears fruit, models are likely the only current option for estimating mountain SWE across large spatial scales.

Recent work with regional climate models (RCMs), particularly the Weather Research and Forecasting (WRF) model, suggests that RCM simulations accurately reproduce realistic snowpack characteristics in mountain regions (Berg & Hall, 2017; Caldwell et al., 2009; Jin & Wen, 2012; Liu et al., 2017; Minder et al., 2016; Pavelsky et al., 2011; Qian et al., 2010; Rasmussen et al., 2011; Waliser et al., 2011; Wrzesien et al., 2015; Wrzesien et al., 2017). Model advancements have specifically targeted improved modeling of SWE and snowfall through incorporating multilayer snowpacks (Etchevers et al., 2004; Niu et al., 2011) and better representation of snowflakes in microphysics schemes (Thompson et al., 2008). Wrzesien et al. (2017) compared snow water storage (SWS) estimates—the equivalent volume of water held as snow—for the Sierra Nevada in California from global/continental models and WRF simulations to reference data sets, which approximated the best guess for actual SWS conditions. They showed that WRF estimates at 9-km spatial resolution were within ±27% of a reference average maximum SWS based on the best observationally constrained data sets, defined as the Sierra Nevada Snow Reanalysis (SNSR; Margulis et al., 2016), the Snow Data Assimilation System (SNODAS; Carroll et al., 2001), and a spatial interpolation of snow course measurements. Global/continental data sets underestimated maximum SWS by up to 88%. Often run at much finer spatial resolutions than global models, RCMs like WRF can capture orographic precipitation processes, which are essential for simulating snowfall in mountain regions.

Due to their computational requirements, however, RCMs are not run globally and generally run for only a few years, rather than a typical 30-year climatology. In order to estimate global mountain SWS, global data sets must be used. However, it is difficult to evaluate snowpack characteristics estimated from global data products since no spatiotemporal truth data set exists for SWE. Instead, model intercomparisons are performed in order to determine whether there is a consensus among models or whether they reach dramatically different conclusions. Recent studies have compared model-estimated SWS in regions across the globe (Broxton et al., 2016; Mudryk et al., 2015; Snauffer et al., 2016; Terzago et al., 2014; Terzago et al., 2017). Though previous work has evaluated global data sets across mountains, they are often limited to a single region. Here we expand previous model intercomparisons by evaluating modeled snow accumulation across the global mountains. However, we first need a common spatial reference delineating the extent of seasonal snow accumulation in global mountains.

To support analysis of global mountain snow, we present a new data product, the Seasonal Mountain Snow Mask (SMSM), combining a digital elevation model (DEM) and remote sensing observations, that classifies seasonally snow-covered mountain regions of the globe. Produced at high spatial resolution (30 arc sec, approximately 1 km at the equator), we use the SMSM to estimate mountain SWS using four global hydroclimate data sets: two reanalyses and two offline land surface models. Uncertainty in the state of mountain SWS is largely unconstrained (Mudryk et al., 2015). As such our primary research question is the following: How do snow accumulation estimates differ among multiple global data sets? Specifically, is there a larger consensus among estimates of total snow accumulation versus estimates of snow accumulation over mountain regions? We hypothesize that global estimates will have less agreement over mountain regions, since it is challenging to model mountain snow accumulation (Bormann et al., 2018; Broxton et al., 2016; Mudryk et al., 2015; Snauffer et al., 2016; Wrzesien et al., 2017). We also compare the global estimates of SWS to multiple regional data sets, all of which have been evaluated in previous studies with regards to their ability to simulate snow. If the global data sets disagree with each other or with the regional data sets, that could suggest limitations in our ability to accurately represent water budgets on global scales.

2. Data and Methods

2.1. SMSM

Despite the importance of mountain snow accumulation, we lack a consensus definition of what constitutes a mountain across the hydrological sciences. Previous studies classify mountains based on elevation (Messerli & Ives, 1997), by standard deviation of local elevation (Takala et al., 2011), or by relief roughness (Körner et al., 2011; Meybeck et al., 2001). Kapos et al. (2000) define mountains based on elevation, slope,

and local relief. Each definition classifies a differing percentage of the global land area as mountainous (Table 1), with values ranging from 12% to 39%. Here, we follow the method developed by Kapos et al. (2000), which has been used in other recent studies (Blyth et al., 2002; Huddleston et al., 2003; Platts et al., 2011). In the Kapos et al. (2000) definition, a DEM grid cell is mountainous in any of the following situations:

1. Elevation ≥2,500 m
2. Elevation 1,500–2,500 m and slope >2°
3. Elevation 1,000–1,500 m and slope >5° or local relief >300 m
4. Elevation 300–1,000 m and local relief >300 m,

where local relief is based on elevations of all DEM grid cells in a 7-km radius around the grid cell of interest. We use the United States Geological Survey's Global 30 Arc-Second Elevation (GTOPO30) DEM, which is the same DEM used by Kapos et al. (2000) in their classification.. Figure 1a shows a map of global mountains with the Kapos et al. (2000) definition. Here we create a raster data set for mountain regions; if readers are interested in polygons to define individual mountain ranges, we suggest the Körner et al. (2017) data set.

Though both Greenland and Antarctica have mountains, the Kapos et al. (2000) definition also classifies ice sheets as mountains; to focus on snow in the context of land surface hydrology, we exclude all of Greenland and Antarctica from our analysis. As with any global classification, this definition may not capture all small-scale mountain features (Browne et al., 2004; Viviroli & Weingartner, 2004); however, the Kapos et al. (2000) classification is not too strict, as it includes high mountain plateaus, unlike the Körner et al. (2011) definition, nor is it too generous, as it excludes hills and plateaus from medium altitude regions, unlike the Viviroli et al. (2007) definition (Table 1).

Next, we determine where seasonal snow is likely to accumulate. We use the duration of snow cover to differentiate seasonal from ephemeral snow. We follow Sturm et al. (1995), who classify snow as ephemeral if it persists for less than 2 months; snow that remains on the ground longer than two consecutive months is seasonal. We are most interested in measuring seasonal snow extent because it captures areas where snow accumulation acts as a natural water reservoir throughout the cool season.

We use the Moderate Resolution Imaging Spectroradiometer (MODIS; Justice et al., 1998) MOD10A2 version 6 product, with a spatial resolution of 500 m, to determine the location and persistence of snow (Hall et al., 2002; Hall & Riggs, 2016). MOD10A2 is a binary snow cover product that reports the maximum snow extent over 8-day periods, as calculated from daily MOD10A1 estimates of snow cover fraction. If snow is present during any of the 8 days, the grid cell is classified as snow in the MOD10A2 product. If there is no snow, the grid cell is classified as the most common clear-view observation (i.e., land, ocean, or lake). If all 8 days are obscured by clouds, the grid cell is classified as cloud.

We use MOD10A2 data for a total of 16 water years (2001 through 2016) to identify seasonal and ephemeral snow. For each water year, at least seven consecutive MOD10A2 8-day periods must have snow cover (for a total snow duration of 56 days) to classify a grid cell as seasonal snow, approximating the 60-day threshold between ephemeral and seasonal snow common in the literature (Petersky & Harpold, 2018; Sturm et al., 1995). We also identify grid cells that have a least 32 days of snow cover and classify them as ephemeral snow. Once we have performed this analysis for all grid cells in a single water year, we repeat for all water years. If a grid cell has seasonal snow for at least eight water years (≥50% of the MOD10A2 record), we define the grid cell as seasonal snow (Figure 2). Similarly, if a grid cell has ephemeral snow for the majority of the MODIS record (at least eight water years), we classify it as ephemeral. Repeating for all grid cells in all granules creates our seasonal snow mask. We assume that any snow-covered grid cells that do not meet at least the 32-day consecutive snow cover threshold are too transient in nature to substantially alter the seasonality of runoff and are not included in our analysis, although we recognize that such transient snow affects soil moisture and vegetation in the mountains. We tested the same analysis with the MYD10A2 data set from the MODIS/Aqua satellite; since the results were nearly identical, we used MOD10A2 for its longer temporal record.

Mountainous regions are frequently cloudy during the winter, particularly during snow accumulation. For each hemisphere, we identify regions with cloudy conditions throughout the cool season (October through March for the North Hemisphere and April through September for the Southern Hemisphere) by summing

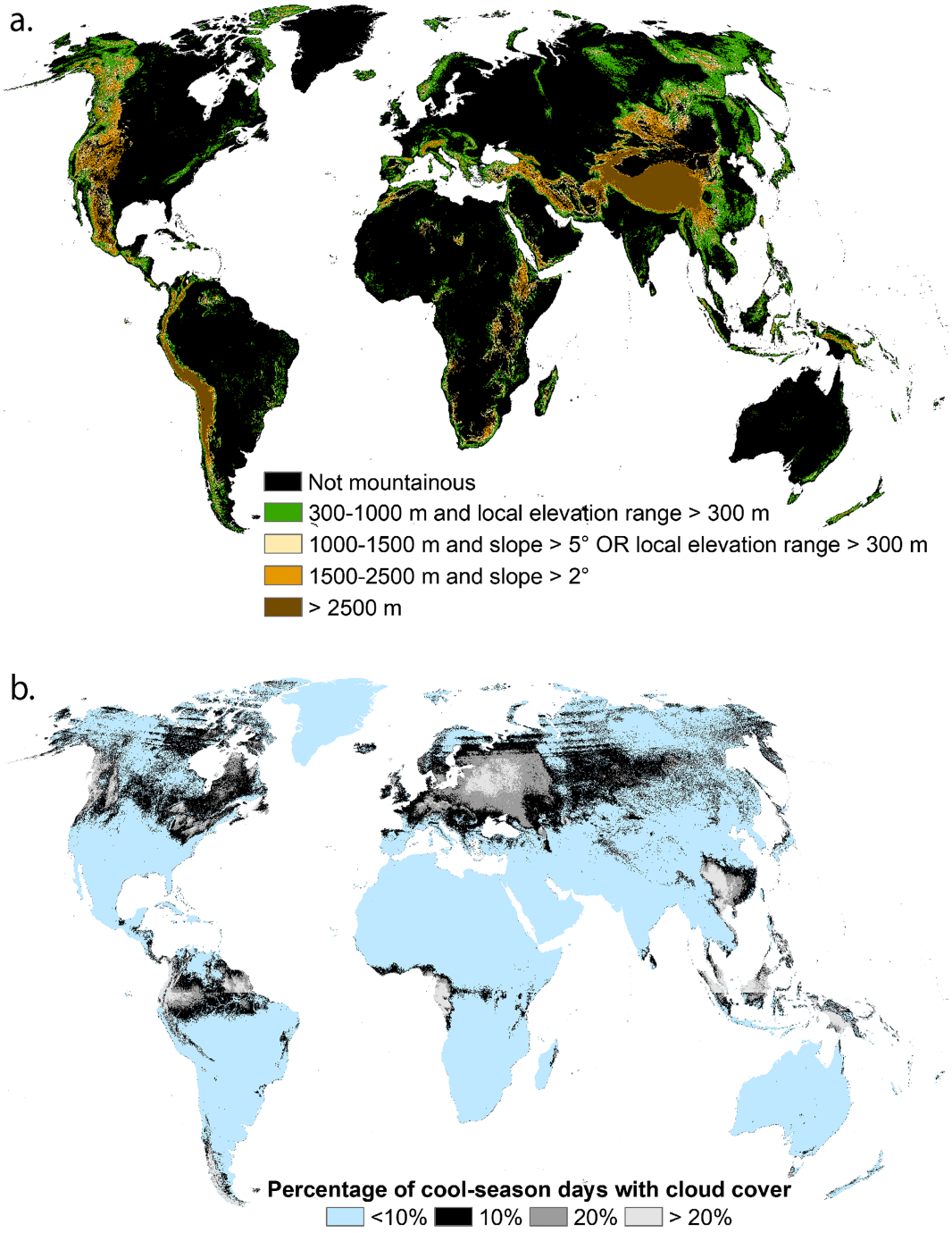

Figure 1. (a) Elevation, slope, and local elevation range criteria for global mountain classification. Black areas indicate non-mountainous regions. (b) Regions with cloud cover for at least 10% of the cool season (October through March for the Northern Hemisphere and April through September for the Southern Hemisphere). Lighter gray colors indicate regions with a higher percentage of days with cloud cover.

the number of MOD10A2 periods with 8 days of consecutive cloud cover (Figure 1b). Persistent cloud cover obscures the ground from view of the MODIS sensor; therefore, we cannot determine whether the ground is snow-covered or bare. If a grid cell has cloud cover for at least 10% of the cool season (at least two 8-day MOD10A2 periods of cloud cover) and no evidence of consecutive snow cover, we label it as "indeterminate due to clouds" and do not include it in our SMSM. We remove all indeterminate areas

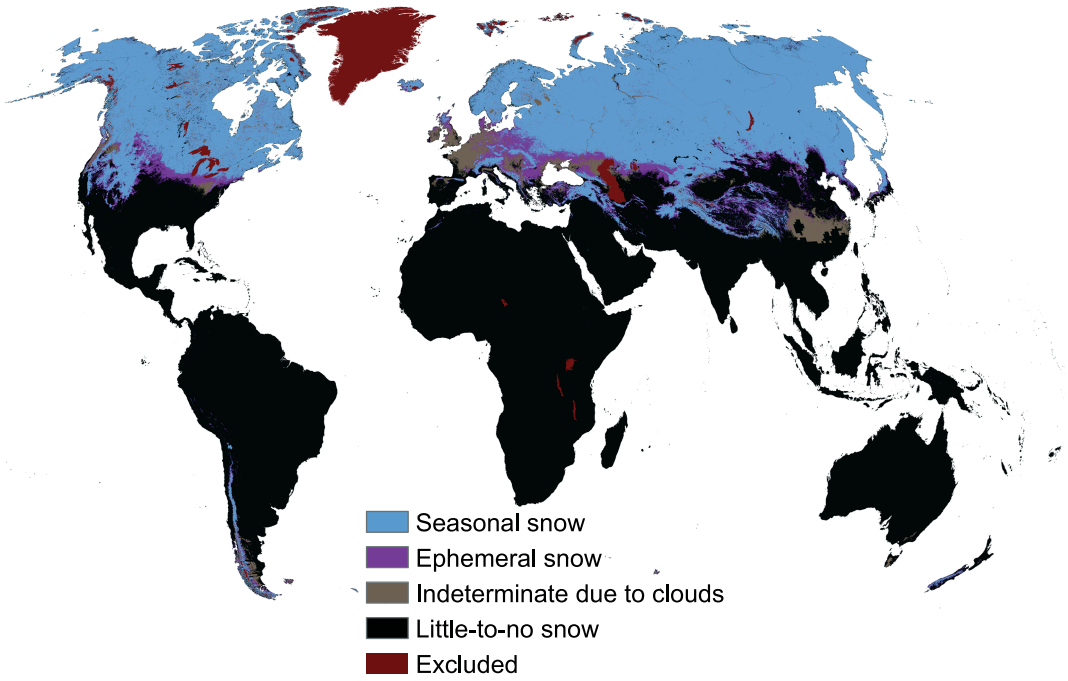

Figure 2. Global mask for where seasonal and ephemeral snow accumulates, from Moderate Resolution Imaging Spectroradiometer snow extent imagery. Regions with persistent cloud cover, which prevents the sensor from determining whether the surface is snow covered, are shown in brown. Large lakes, glaciers, and Greenland, which are excluded from the analyses, are shown in red.

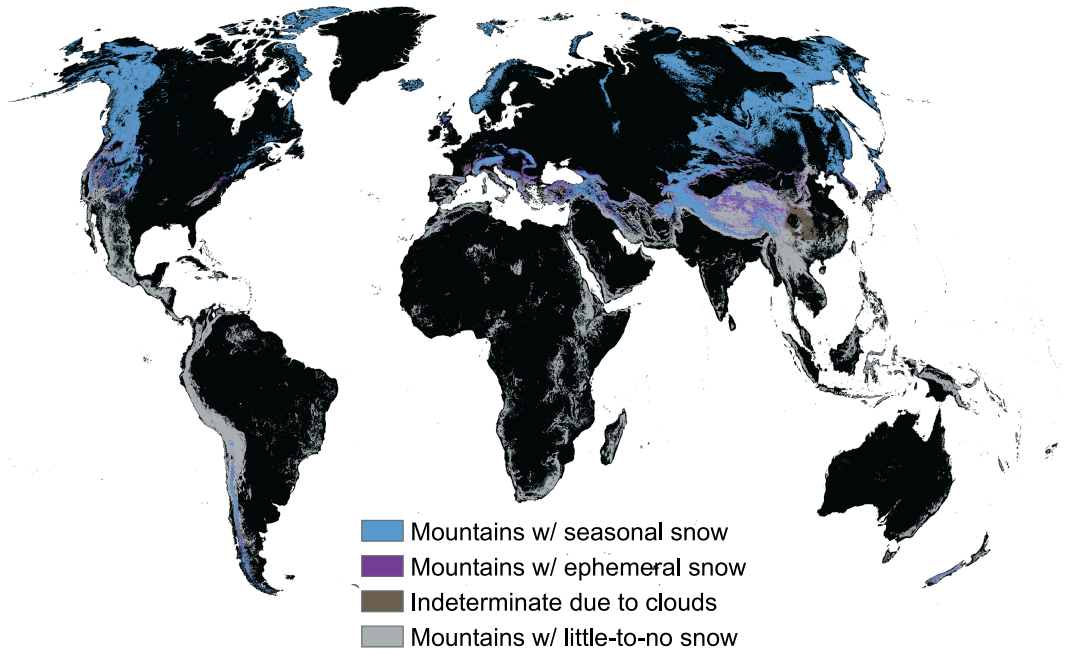

Figure 3. The Seasonal Mountain Snow Mask: A classification of global mountains that support a seasonal snowpack, shown in blue. Regions with ephemeral snow cover are shown in purple. Regions with persistent cloud cover, which prevents the sensor from determining whether the surface is snow covered, are shown in brown.

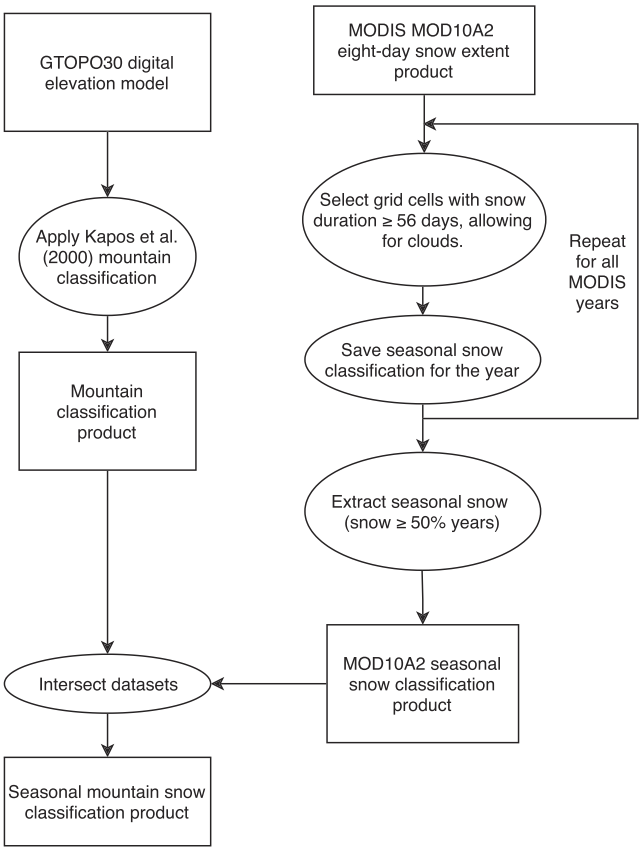

Figure 4. Flow chart to describe the process of combining a mountain classification from GTOPO30 digital elevation model with a seasonal snow classification MODIS to produce the seasonal mountain snow classification data product. In the flow chart, data sets are indicated with boxes and processes with ovals. MODIS = Moderate Resolution Imaging Spectroradiometer.

that have an average temperature of −5 °C for the coldest month of the climatology (supporting information Figure S1), as calculated from Modern-Era Retrospective Analysis for Research and Applications (MERRA)-2 monthly surface temperature estimates from 1980–2016, since we can assume these regions, mostly in the tropics, do not accumulate snow. However, if a grid cell has cloud cover for at least 10% of the cool season but also has enough clear-sky observations of snow cover, it can still be classified as seasonal or ephemeral snow.

To allow for cloudy conditions during periods of snow accumulation, we assume that if two snow-covered MOD10A2 observations bracket one or more cloudy MOD10A2 observations, the cloudy period is likely snow covered, too. Following this assumption, we require only the first and last 8-day MOD10A2 observations to be snow covered. That is to say, if we have one snowy MOD10A2 observation, five cloudy MOD10A2 periods, and one snowy observation, we classify the 56-day period as snow covered. Similarly, for the ephemeral snow grid cells, we allow for two periods of cloudy conditions to occur between two MOD10A2 snow-covered observations. We acknowledge this assumption adds uncertainty to our method; wintertime clouds do not always obscure snow-covered ground. In test cases where we did not allow interpolation over cloudy periods, our estimates of snow-covered area were often dramatically lower (see Figure S2) due to persistent cloud cover. By allowing for cloudy conditions to fall within snow-covered observations, we capture regions that are frequently cloudy during the winter yet also have seasonal snow cover, such as the Cascade Range in the Pacific Northwest of the United States.

In addition to the assumption that we can interpolate over cloudy images, we also assume that when MOD10A2 classifies a grid as snowy, all days have snow cover. This is not always true; MOD10A2 shows the maximum snow extent, so it is possible for only a single day over the 8-day period to have snow cover. However, we use the MOD10A2 8-day product since it does not require as much data storage or computation time as the daily MOD10A1 data set. Since MOD10A2 incorporates multiple days into each observation period, it provides a smoother time series and reduces the need for postprocessing missing observations, whether due to orbit gaps or cloud cover (Figure S3). Additionally, MOD10A1 has variable angular viewing over the 16-day repeating ground track that increases the amount of necessary postprocessing.

We combine the global mountain (Figure 1a) and seasonal snow cover maps (Figure 2) to create the SMSM (Figure 3). That is, we select the mountainous areas that also have seasonal snow cover for ≥50% of water years 2001–2016. The steps in the process, including classifying mountain regions and seasonal snow cover regions, are detailed in Figure 4. The SMSM is produced at 30-arc sec spatial resolution to match the GTOPO30 resolution, though it could easily be aggregated to different spatial resolutions. The SMSM and the cloud product are available on Google Earth Engine (https://code.earthengine.google.com/?asset=users/melissawrzesien/MODIS_snowClassification) and are available for download from Zenodo (Wrzesien, Pavelsky, et al., 2019).

2.2. Global Data Products

We perform a model intercomparison to evaluate how mountain SWS varies among global data sets. Using the SMSM to identify seasonally snow-covered mountains, we compare mountain SWS climatological estimates from four global data sets:

1. the European Centre for Medium-Range Weather Forecasts Reanalysis (ERA-Interim; Dee et al., 2011)
2. the Global Land Data Assimilation System (GLDAS; Rodell et al., 2004) version 2.0
3. the MERRA (Rienecker et al., 2011) version 2

4. the Variable Infiltration Capacity hydrologic model (VIC; Liang et al., 1994) version 4.0.3 (Nijssen, O'Donnell, Hamlet, & Lettenmaier, 2001; Nijssen, O'Donnell, Lettenmaier, et al., 2001; Nijssen, Schnur, & Lettenmaier, 2001).

For ERA-Interim, GLDAS, and MERRA-2, we calculate average annual SWS over 1980–2010, a 31-year climatology. Due to data availability, we only have a 14-year climatology (1980–1993) for VIC. Further details about each global data set are available in Table 2. We note that each global data set is much coarser than the native resolution of the SMSM. By necessity, data sets with coarse spatial resolution must average topography. For the mountain SWS evaluation, we select all regions defined as mountainous in the SMSM; this allows us to have a relatively consistent comparison region among the four data sets, where the snow-covered mountain area for each data set is within 9% of the four–data set average.

2.3. Model Intercomparison

2.3.1. Global Comparisons

For each model, we examine the total amount of snow stored globally and in seasonally snow-covered mountains. Since we are interested in seasonal snow accumulation and not permanent snow and ice, we exclude glaciated grid cells, as defined in the Randolph Glacier Inventory (Pfeffer et al., 2014; RGI Consortium, 2017), which provides a global inventory of glacier outlines and is available as shapefiles from the Global Land Ice Measurements from Space initiative (Raup et al., 2007). Figure S4 shows the regions excluded from each global data set. We test multiple glacier thresholds, and we ultimately remove all grid cells >25% glaciated (Table S1); we remove the largest area from GLDAS (613,215 km^2) and the smallest area from VIC (453,318 km^2), with an average area removed of 559,461 km^2. Though a 10% glacier threshold had slightly more agreement between the four global data sets (Table S1), it was too restrictive and removed >1% of land area, while the 25% threshold removed <0.5%. Other recent studies concerned with seasonal snow have also excluded glaciers from their analysis (Mudryk et al., 2015; Wrzesien et al., 2018).

2.3.2. Regional Comparisons

Though we cannot perform a global validation with the four global data sets, we can do regional evaluations. For these regional comparisons, we focus on North America and several regional data sets at higher spatial resolution. For the contiguous United States (CONUS), we compare a higher-resolution VIC simulation that has been adjusted for orographic effects (Livneh et al., 2013); we refer to this data set as VIC/Livneh. The VIC/Livneh simulation has been used in multiple hydroclimatic studies, including in Li et al. (2017) to estimate how much of runoff in the western United States is derived from snow accumulation. We also include a high-resolution (4 km) 13-year WRF simulation from the National Center for Atmospheric Research (Liu et al., 2017; Rasmussen & Liu, 2017), which is available over CONUS; we refer to this data set as WRF/NCAR (National Center for Atmospheric Research). WRF/NCAR simulates water years 2001–2013. Inclusion of this data set allows us to evaluate WRF over a large geographic area for multiple years. Finally, for CONUS, we also use SWE estimates from SNODAS. We caution that SNODAS has been shown to perform poorly when compared to independent measurements of spatially distributed SWE in mountainous regions (Bair et al., 2016; Clow et al., 2012; Hedrick et al., 2015). However, it is commonly used across the literature as an evaluation metric for snow accumulation; we have used SNODAS in previous work to evaluate WRF simulations (Wrzesien et al., 2017; Wrzesien et al., 2018). We include it here for completeness, though we caution that SNODAS has considerable limitations.

For North America, we also consider a second WRF data set, a new representative climatology of SWS created from 9-km WRF simulations (Wrzesien et al., 2018). This WRF data set was created by simulating a single representative year for each mountain range across North America; the selected year approximates the long-term average, as determined by comparing several global and continental estimates (see supporting information of Wrzesien et al., 2018). While the data set approximates the climatological SWS for the continent, it is not a true climatology. When comparing this data set, whether for the continental representative climatology or for individual mountain ranges, we refer to it as WRF/Rep.

As discussed above, numerous recent studies report that WRF demonstrates skill in simulating realistic snow accumulation in mountain regions. Estimates of temperature, precipitation, and SWE from the WRF/NCAR data set were evaluated against both in situ observations and satellite observations (Liu et al., 2017), and WRF/NCAR has been used in multiple studies (e.g., Musselman et al., 2017; Musselman et al., 2018; Prein et al., 2017). In creating their new estimate of North American mountain SWS,

Table 1
Previous Mountain Definitions and Percentage of Land Area Classified as Mountain

Study	Definition	Mountain percentage
Meybeck et al. (2001)	Elevation and relief roughness = $elev_{max} - elev_{min}$/ (1/2 cell length)	25%
Körner et al. (2011)	"Ruggedness"—elevation difference within a defined area	12.3%
Kapos et al. (2000; used here)	Elevation, slope, local relief	27%
Viviroli et al. (2007)	Meybeck et al. (2001) plus all areas above 1,000 m above sea level plus those areas between 200 and 1,000 m above sea level with a relief roughness of more than 20‰	39%

Wrzesien et al. (2018) evaluate WRF simulations against snow pillow observations, SWE estimates from SNODAS, and terrestrial water storage anomaly estimates from the Gravity Recovery and Climate Experiment satellite (GRACE; Tapley et al., 2004; Wahr et al., 2004; Syed et al., 2009, 2010) and conclude that WRF SWS estimates are more reasonable than previous global/continental estimates for North America. More details on the WRF/Rep setup, including model evaluation, are provided by Wrzesien et al. (2018), and their WRF SWS estimates are available at the National Snow and Ice Data Center (Wrzesien & Durand, 2018). However, we caution that WRF is a model and, like the other global data products included in this study, has limitations and uncertainties. Though we do not consider either WRF/NCAR or WRF/Rep to be the truth, a consensus in the literature does indicate that WRF simulations can capture realistic snow characteristics in mountains. Moreover, neither SNODAS nor GRACE provides a robust estimate of snow in the mountains. The most rigorous comparisons of SNODAS with spatially available SWE values show inconsistent performance from year to year (Bair et al., 2016) and missing snow in areas with few snow pillow data to assimilate (Dozier et al., 2016). GRACE has such a large footprint that it cannot distinguish snow from groundwater. Thus, in North America, WRF is likely at least as reliable as the other available data sets that cover the whole area, so we are comfortable evaluating the global data sets against WRF for North America in order to gauge the performance of the global estimates.

To evaluate global and regional estimates of SWS, we compare estimates of SWS for the Sierra Nevada, Cascades, the U.S. Rocky Mountains, and CONUS from WRF/NCAR, VIC/Livneh, SNODAS, WRF/Rep, ERA-Interim, GLDAS, and MERRA-2; we also compare to SNSR over the Sierra Nevada. Since WRF/Rep is only available for one representative water year in each mountain range, we only compare it over water year 2009 for the Sierra Nevada and Cascades and water year 2006 for the U.S. Rockies. We compare all other products for water years 2004 through 2010, to match overlap of when all data sets are available (SNODAS

Table 2
Details and References forGlobal Datasets Used in This Study

Data Set	Spatial resolution	Time period in this study	Precipitation forcing data	Reference
ERA-Interim	~80 km × 80 km	1980–2010	Based on temperature and humidity information from assimilated observations. A full list of assimilated data is available in Dee et al. (2011)	Dee et al. (2011)
GLDAS version 2.0	0.25° × 0.25°	1980–2010	Global Meteorological Forcing Data set from Princeton University (Sheffield et al., 2006)	Rodell et al. (2004)
MERRA-2	0.5° × 0.625°	1980–2010	NOAA Climate Prediction Center (CPC) Unified Gauge-Based Analysis of Global Daily Precipitation (CPCU; Xie et al., 2007; Chen et al., 2008) and the CPC Merged Analysis of Precipitation (CMAP; Xie & Arkin, 1997)	Rienecker et al. (2011)
VIC version 4.0.3	2° × 2°	1980–1993	>7,500 station observations from the CPC	Nijssen, O'Donnell, Hamlet, & Lettenmaier, 2001, Nijssen, O'Donnell, Lettenmaier, et al., 2001, Nijssen, Schnur, & Lettenmaier, 2001)

Note. ERA = European Centre for Medium-Range Weather Forecasts Reanalysis; GLDAS = Global Land Data Assimilation System; MERRA = Modern-Era Retrospective Analysis for Research and Applications; VIC = Variable Infiltration Capacity; NOAA = National Oceanic and Atmospheric Administration.

Table 3
Mountain and Seasonally Snow-Covered Mountain Area by Continent

Continent	Continental land area (km^2)	Mountain area (km^2)	Continental mountain percentage (%)	Seasonally snow-covered mountain area (km^2)	Percentage of mountains with seasonal snow cover (%)	Seasonally snow-covered area (km^2)	Snow-covered mountains as a percentage of total snow-covered area
Africa	29,872,396	3,384,276	11.3	5,319	0.2	5,982	88.9
Asia	44,731,080	15,878,572	35.5	7,505,717	47.3	19,591,382	38.3
Australia	8,074,387	407,408	5.0	39,705	9.7	42,586	93.2
Europe	9,861,865	1,632,907	16.6	833,552	51.0	5,750,038	14.5
North America	21,977,778	5,515,901	25.1	3,416,767	61.9	12,819,510	26.7
South America	17,674,496	3,141,978	17.8	260,339	8.3	318,838	81.7
Global	132,192,002	29,961,042	22.7	12,061,399	40.3	38,528,336	31.3

begins in 2003 and GLDAS ends in 2010). The global VIC product is not included since the version used here is only available through 1993.

3. Results

Prior to evaluating estimates of SWS, we first identify mountains with seasonal snow cover. The global mountain area is 30.0×10^6 km^2, excluding Greenland and Antarctica (Figure 1a). The seasonally snow-covered area is 38.7×10^6 km^2 (Figure 2), 29% of the global land area. When selecting the seasonally snow-covered mountains with the SMSM, seasonal mountain snow covers 12.1×10^6 km^2, 40% of total mountain area and 31% of the total snow-covered area (Figure 3). Ephemeral mountain snow covers an additional 1.6×10^6 km^2, 5% of total mountain area. Mountains cover 23% of the Earth's land area, while seasonally snow-covered mountains cover 9%. Three percent of global mountains (<1% of Earth's land area) cannot be accurately classified as seasonal snow, ephemeral snow, or little-to-no snow due to clouds obscuring the land surface. We also separate mountain and snow-covered mountain area by continent for regions with seasonal (Table 3) and ephemeral snow (Table S2). The mountain land area in Asia is nearly 3 times larger than the next continent (North America). In North America, 62% of mountains accumulate seasonal snow. Africa has the smallest ratio of snowy mountains (0.15%), while Australia has the smallest mountain area.

Using the SMSM, we compare daily climatological SWS for each hydroclimate data set over global land, snow-covered mountain, and lowland areas (Figure 5); we define lowland as nonmountainous regions (shown in black in Figure 1a). The largest difference in total global SWS occurs in March, where the climatological maximum values range from 2,861 km^3 from GLDAS to 5,540 km^3 from VIC, nearly 2 times larger than the GLDAS estimate (Table 4). The climatological maximum SWS from all four estimates is within ±36% of the four–data set mean. Throughout the full time series (Figure 5a), VIC and MERRA-2 always have the largest values of SWS, while GLDAS is always smallest. When comparing the interannual variability of each data set (Figure S5), MERRA-2 has the largest range in annual maximum SWS, where the difference between the largest maximum and the smallest is 1,272 km^3 (Table S3), and VIC has the smallest range in maximum SWS (553 km^3). Most of the range in the MERRA-2 values is due to a single water year (water year 1982) with 456 km^3 more SWS than the next highest year. The other three global data sets have larger standard deviations in maximum SWS compared to MERRA-2, where MERRA-2 has a standard deviation of 150 km^3 and ERA-Interim, GLDAS, and VIC have values of 191, 242, and 170 km^3, respectively. The four data sets fall into two categories for average day-of-peak SWS over their periods of record; ERA-Interim and GLDAS peak earlier (28 February for ERA-Interim and 5 March for GLDAS), while MERRA-2 and VIC peak later (18 March for MERRA-2 and 21 March for VIC). VIC has the smallest standard deviation of day-of-peak SWS (3 days), while ERA-Interim has the largest (7 days). We also consider whether each data set identifies the same high and low snow accumulation years (Figure S6). For global SWS, the greatest agreement is between VIC and MERRA-2 and between VIC and GLDAS. ERA-Interim does not appear to have similar interannual variability to any of the other data sets.

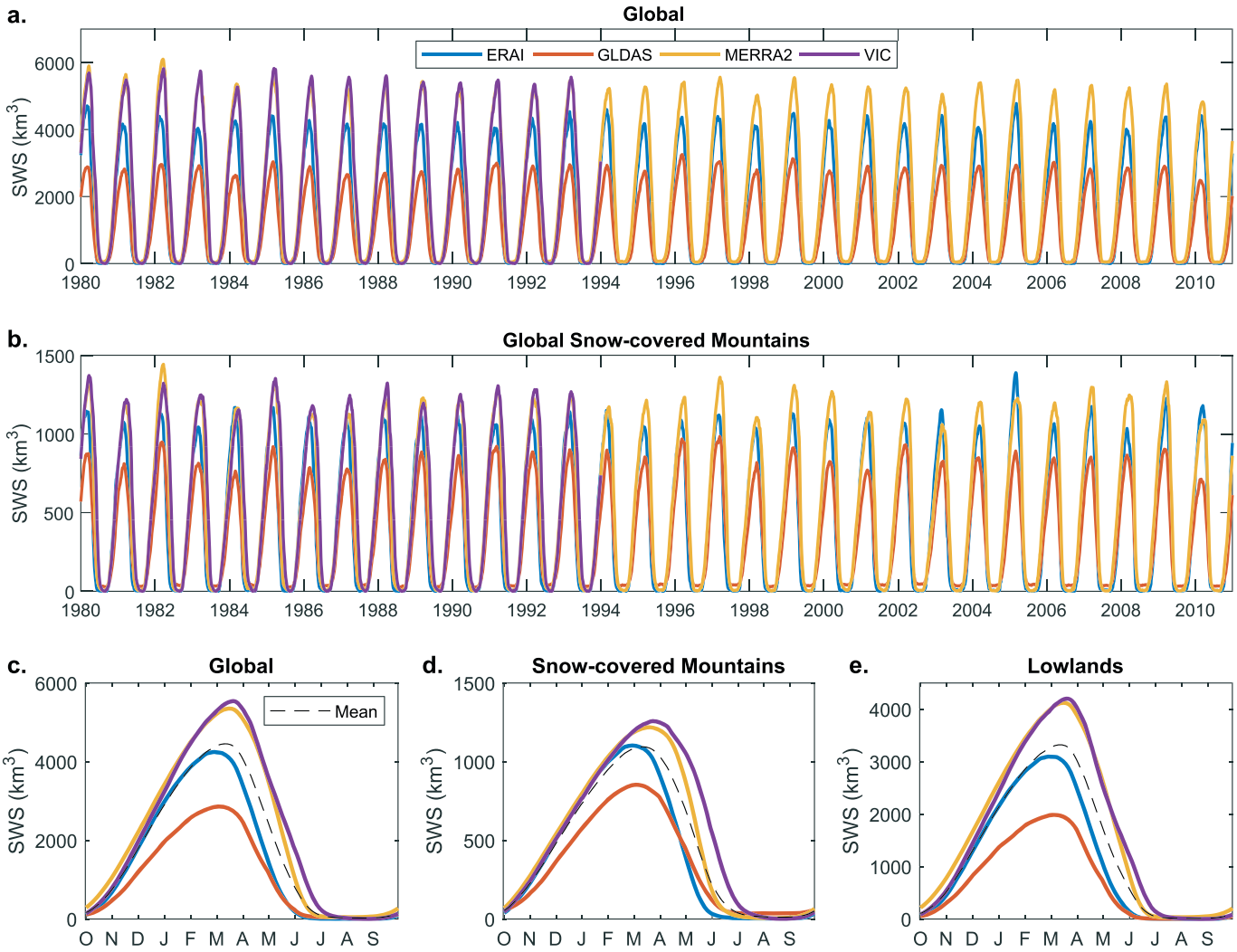

Figure 5. (a) Full time series of snow water storage, in cubic kilometers, from all four global data sets for all seasonal snow. (b) Time series of snow water storage, in cubic kilometers, for seasonally snow-covered mountain ranges. (c) Average climatological daily snow water storage, in cubic kilometers, for each global data set. (d, e) Same as (c) but for only the seasonally snow-covered mountains and lowlands of the globe, respectively. ERAI = European Centre for Medium-Range Weather Forecasts Reanalysis Interim; GLDAS = Global Land Data Assimilation System; MERRA = Modern-Era Retrospective Analysis for Research and Applications; VIC = Variable Infiltration Capacity; SWS = snow water storage.

When comparing across the seasonally snow-covered mountain regions, there is a stronger consensus among the four global data sets regarding maximum SWS: The largest estimate (VIC with 1,258 km^3) is ~1.5 times larger than the smallest (GLDAS with 853 km^3). Each data set is within ±23% of the four–data set average for maximum mountain SWS (Figure 5b). On average, seasonal SWS in mountains accounts for 25% of the total global SWS. We note that though seasonally snow-covered mountains are 40% of total mountain area, nearly all the mountain SWS is within the regions we flag as seasonally snow-covered (Table S4). Across nonmountain lowland regions, GLDAS is 41% lower than the four–data set average, though the other estimates are within ±25% of the average (Figure 5c). By comparing maximum SWS from each year between data sets (Figure 6), we can determine whether the global products identify the same high and low snow accumulation years. MERRA-2, GLDAS, and VIC have Pearson correlations ?0.68, suggesting the year-to-year SWS variations are similar. ERA-Interim, however, is the exception; it does not have similar variability with any of the other data sets. While SWS magnitudes from ERA-Interim may be comparable to MERRA-2 or VIC (GLDAS tends to have less SWS), they do not agree with ranking high or low snow accumulation years.

Table 4
Snow Water Storage (SWS), Globally and by Continent, From Each Global Data Product, Measured in Cubic Kilometers

Continent	Total land vs. snow-covered mountain	ERA-Interim	GLDAS	MERRA-2	VIC	Average
Global	All land	4,247	2,861	5,350	5,540	4,500
	Snow-covered mountain	1,103 (26%)	853 (30%)	1,219 (23%)	1,258 (23%)	1,108 (25%)
Africa	All land	<1	<1	<1	1	<1
	Snow-covered mountain	<1	<1	<1	<1	<1
Asia	All land	1,969	1,172	1,897	2,790	1,957
	Snow-covered mountain	636 (32%)	403 (34%)	586 (31%)	726 (26%)	588 (30%)
Australia	All land	<1	5	1	<1	1
	Snow-covered mountain	<1	3	<1	<1	1
Europe	All land	706	650	800	1,215	843
	Snow-covered mountain	107 (15%)	134 (21%)	127 (16%)	76 (6%)	111 (13%)
North America	All land	1,492	1,011	1,627	1,537	1,417
	Snow-covered mountain	36 (25%)	299 (30%)	505 (31%)	461 (30%)	408 (29%)
South America	All land	15	12	14	28	17
	Snow-covered mountain	7 (47%)	7 (62%)	3 (23%)	1 (3%)	5 (27%)

Note. Values in parentheses indicate the percentage of global/continental SWS that accumulates in seasonally snow-covered mountains. ERA = European Centre for Medium-Range Weather Forecasts Reanalysis; GLDAS = Global Land Data Assimilation System; MERRA = Modern-Era Retrospective Analysis for Research and Applications; VIC = Variable Infiltration Capacity.

To evaluate over continents, we only consider Asia, Europe, North America, and South America, since Africa and Australia have negligible SWS (Table 4). Mountains in Asia, Europe, North America, and South America contain an average of 31%, 14%, 29%, and 34% of total continental SWS, respectively. South America, however, differs from the other continents since the percentage of seasonal snow within mountains ranges from 3% (from VIC) to 62% (from GLDAS). Other continents have much smaller ranges (26–34% for Asia, 6–21% for Europe, and 25–31% for North America). Much of the South American land mass is along or near the equator, where warmer temperatures prevent seasonal snow from accumulating; North America and Eurasia, on the other hand, have broad expanses of nonmountain land mass where snow accumulates. These differences in land distribution likely help explain the differences in the percent of snow that accumulates within mountainous areas for each continent. For South America, VIC's estimate may be lower due to its coarse spatial resolution; much of the Andes in South America are less than 200 km wide, narrower than the 2° resolution of VIC.

For mountain SWS in Asia, Europe, and North America, all estimates are within ±32%, ±32%, and ±27% , respectively, of the mean (Figure 7). In South America, VIC is 80% less than the mean, while GLDAS, MERRA-2, and ERA-Interim have much more SWS across the entire year. The agreement between the four global data products is perhaps surprising given the challenges associated with modeling mountain snow (Bormann et al., 2018; Broxton et al., 2016; Mudryk et al., 2015; Snauffer et al., 2016; Wrzesien et al., 2017).

There is no “truth” to compare mountain SWE against at continental scales; thus, we compare modeled SWS, from the global data sets and from WRF, to data products that likely envelope the truth (Figure 8). For the CONUS time series and those for the individual mountain ranges, the regional data sets with high spatial resolution (WRF/NCAR, SNODAS, and VIC/Livneh) estimate larger amounts of SWS than ERA-Interim, GLDAS, or MERRA-2. For the Sierra Nevada, the SNSR is in agreement with all three regional data sets but not the global data sets. Though the accumulation patterns are often similar (e.g., water year 2008 over CONUS), the global data sets generally melt earlier and accumulate far less SWS than the regional data sets. Differences are larger for individual mountain ranges than for CONUS, particularly the Sierra Nevada and the Cascades, both narrow coastal ranges. Assuming the regional data sets, including the SNSR and SNODAS as “reference data sets” from previous studies, are more likely to capture true values of SWS, the time series comparison suggests that global data sets underestimate SWS, particularly in mountain areas. We also show that WRF/NCAR agrees with VIC/Livneh, SNODAS, and SNSR. In addition to previous literature that suggests WRF produces reasonable estimates of SWS (see section 2.3.2), these comparisons indicate that WRF is consistent with other published snow data sets.

We evaluate WRF/Rep and the other regional data sets over the individually chosen water years meant to approximate average snow accumulation conditions (bold years in Figure 8). For water year 2009 in the Sierra Nevada, WRF/Rep's SWS estimate agrees with the reference data sets (maximum WRF/Rep SWS

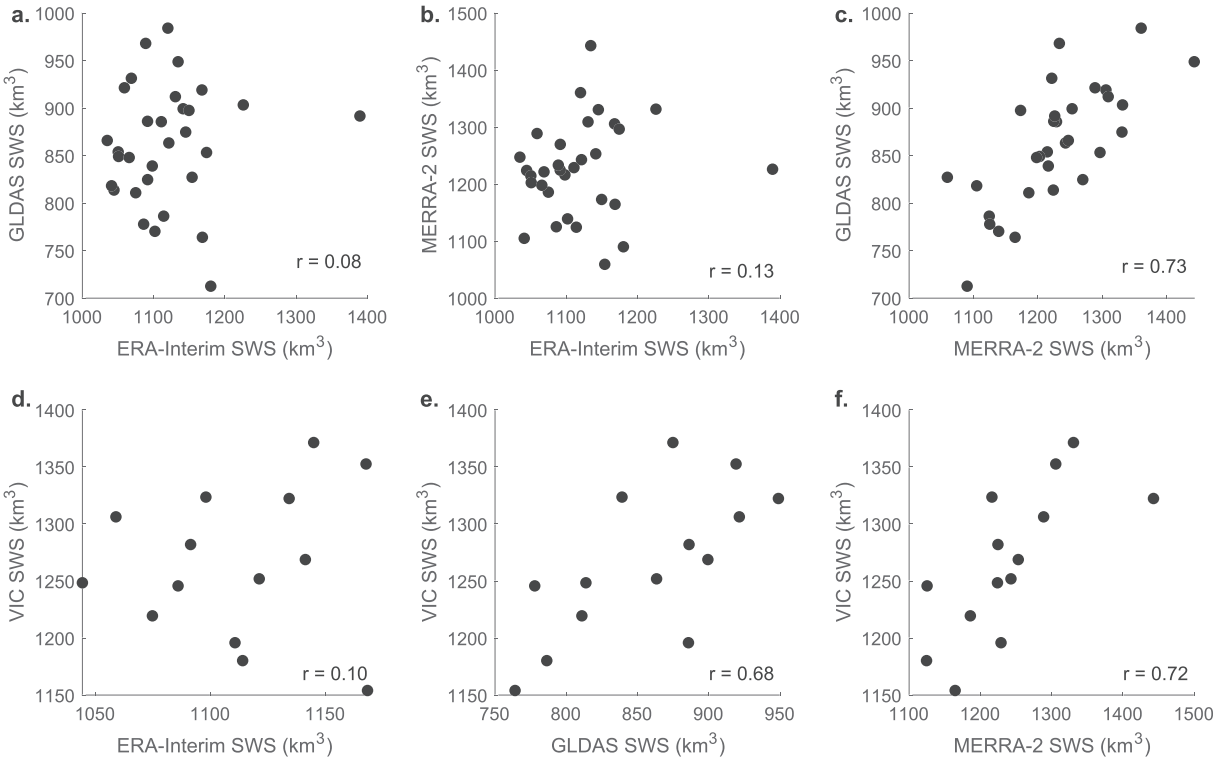

Figure 6. Comparison of annual snow water storage values for seasonally snow-covered mountain areas from each data set. (a–c) Comparisons are over 1980–2010. (d–f) Comparisons are over 1980–1993, due to limitations in availability of VIC data. ERA = European Centre for Medium-Range Weather Forecasts Reanalysis; GLDAS = Global Land Data Assimilation System; MERRA = Modern-Era Retrospective Analysis for Research and Applications; VIC = Variable Infiltration Capacity; SWS = snow water storage.

within 9% of the reference maximum SWS), while the global data sets underestimate the reference maximum SWS by 80–91%. WRF/NCAR maximum SWS for the Sierra Nevada is 18% lower than the reference average. Compared to the VIC/Livneh simulations, WRF/Rep SWS is 5% larger, WRF/NCAR SWS is 5% smaller, and the global data sets underestimate by 77–89%. For water year 2009 in the Cascades, WRF/Rep SWS is 23% larger than SNODAS SWS and WRF/NCAR is 9% smaller than SNODAS, while the global data sets underestimate by 64–77%. VIC/Livneh has the largest SWS estimate for the Cascades, likely caused by a cold bias in the lapse rate (Minder et al., 2010); compared to VIC/Livneh, WRF/Rep SWS is 29% less, WRF/NCAR SWS is 47% less, and the global estimates are 79–87% smaller. Similarly, over the U.S. Rocky Mountains for water year 2006, WRF/Rep overestimates SNODAS SWS by 6%, WRF/NCAR underestimates SNODAS SWS by 10%, and the global data sets underestimate by 61–91%. Compared to VIC/Livneh for the Rocky Mountains, WRF/Rep underestimates SWS by 8%, WRF/NCAR underestimates by 22%, and the global data sets underestimate by 67–93%. Though this comparison encompasses only 1 year for each of three mountain ranges, it suggests both WRF/Rep and WRF/NCAR are more reasonable than the three global data sets. The finding that WRF/Rep in the Sierra Nevada compares within 6% to a rigorous observation-based analysis (Margulis et al., 2016), which in turn is only slightly larger than another independent assessment (Bair et al., 2016), shows that in the Sierra Nevada at least, WRF/Rep is more reliable than SNODAS (within 7% of SNSR). Thus, the differences between WRF estimates and SNODAS in the Cascades and the Rocky Mountains do not show evidence of shortcomings in WRF simulations.

Reference data sets for mountain SWS are not available globally. However, since previous work suggests WRF not only approximates reference data sets over the Sierra Nevada mountains (Wrzesien et al., 2017) but also that WRF shows skill in modeling mountain snow accumulation (Caldwell et al., 2009; Jin & Wen, 2012; Liu et al., 2017; Minder et al., 2016; Qian et al., 2010; Rasmussen et al., 2011; Waliser et al., 2011), we evaluate the SWS estimates from the global data sets against WRF/Rep North American SWS

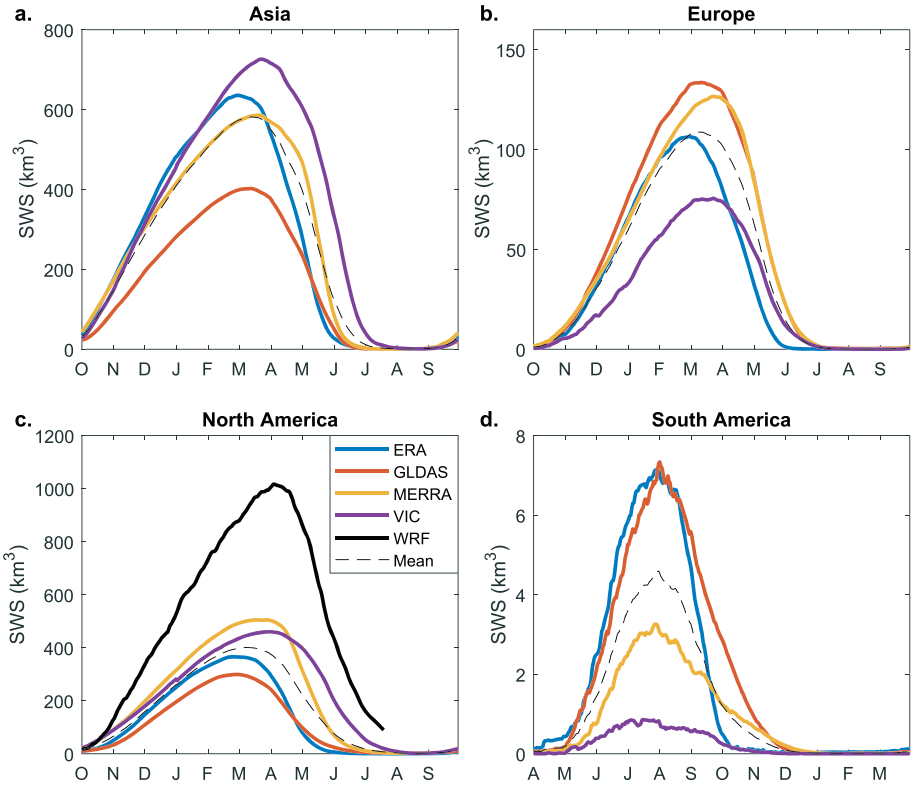

Figure 7. Seasonally snow-covered mountain snow water storage, in cubic kilometers, for each global data product over the water year for (a) Asia, (b) Europe, (c) North America, and (d) South America. Note that the South American water year starts on 1 April. The North America comparison includes a representative climatology from the Weather Research and Forecasting (WRF) regional model (black line). The dashed black line is the mean of the four global data sets. ERA = European Centre for Medium-Range Weather Forecasts Reanalysis; GLDAS = Global Land Data Assimilation System; MERRA = Modern-Era Retrospective Analysis for Research and Applications; VIC = Variable Infiltration Capacity; SWS = snow water storage.

simulations (Wrzesien et al., 2018). WRF/NCAR is only available for CONUS and does not include high-latitude mountain ranges. North America SWS estimates from global data sets are 50–70% lower than the WRF/Rep peak SWS estimate of 1,010 km^3, with an average bias of −60% (Figure 7c). MERRA-2 is the most similar to WRF/Rep, though still 50% lower.

4. Discussion

In this study, we show that global data set estimates of SWS for global land areas range from 2,861 to 5,540 km^3, with all four data sets within 36% of the average SWS of 4,450 km^3. VIC and MERRA-2 have the largest estimates of global SWS and the latest dates of maximum SWS. GLDAS has the smallest SWS, and ERA-Interim has the earliest average day-of-peak SWS. Standard deviations of annual maximum SWS range from 2.8% of average annual value (MERRA-2) to 8.4% (GLDAS). Since the data sets cover different time periods (1980–2010 for ERA-Interim, GLDAS, and MERRA-2 and 1980–1993 for VIC), the full time period could include a climate change signal that is missing from the shorter VIC period. To test whether such differences are likely to affect our results, we compare climatological averages between different periods (Figure S7 and Table S5). We see very little difference between the two time periods. ERA-Interim, GLDAS, and MERRA-2 have similar maximum SWS and day-of-peak SWS for the two time periods. Therefore, while the differences in time period add some uncertainty to the analysis, we do not believe they are likely to impact our conclusions.

Beyond a four–data set intercomparison, we can also evaluate these data sets against other global SWS estimates. We compare to SWS values based on the Sturm et al. (1995) snow classification (Table 5). Using

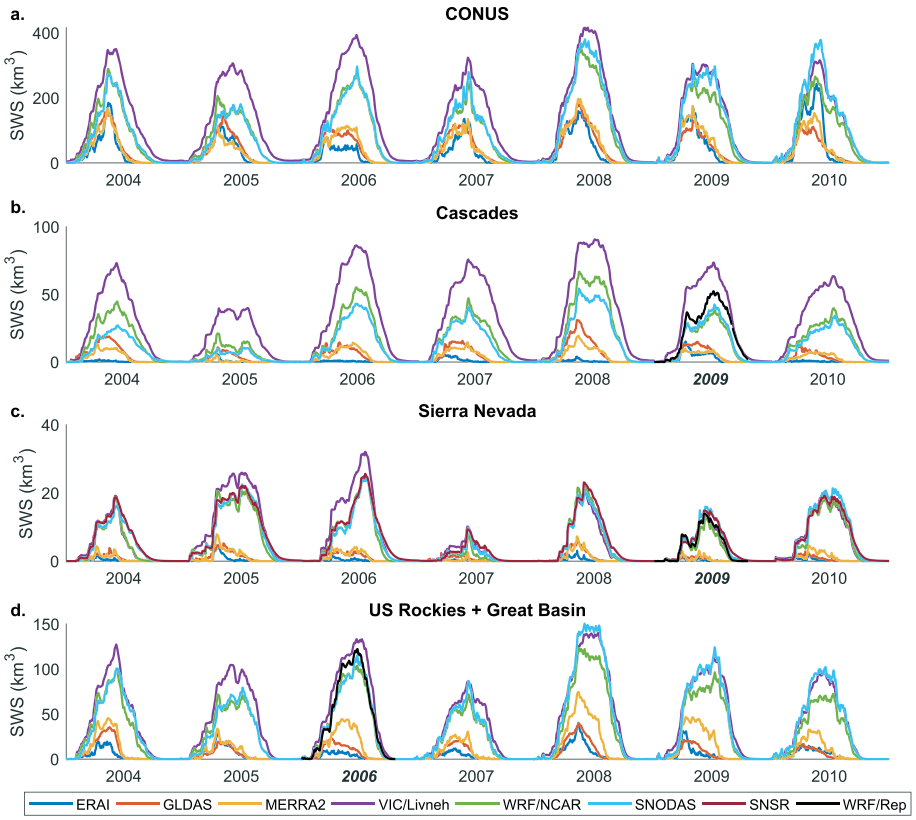

Figure 8. Comparison of snow water storage over (a) the contiguous United States (CONUS), (b) the Cascades, (c) the Sierra Nevada, and (d) the United States Rocky Mountains and the Great Basin for seven water years from global and regional data sets. Bold, italicized years show the representative year from Wrzesien et al. (2018). ERA = European Centre for Medium-Range Weather Forecasts Reanalysis; GLDAS = Global Land Data Assimilation System; MERRA = Modern-Era Retrospective Analysis for Research and Applications; VIC = Variable Infiltration Capacity; WRF = Weather Research and Forecasting; NCAR = National Center for Atmospheric Research; SNODAS = Snow Data Assimilation System; SNSR = Sierra Nevada Snow Reanalysis; SWS = snow water storage.

estimates of average representative snow depth and density from Sturm et al., we calculate the total SWS for the tundra, taiga, and maritime snow cover regions; for these three regions (warm forest and prairie are excluded due to limited information on average snow depth and density), the total global SWS is 5,862 km^3, 29% larger than the four–data set average presented here. Though these values of SWS are somewhat similar, we exclude both warm forest and prairie, with global areas of 3.8×10^6 and 15.5×10^6 km^2, respectively, from our estimate due to limited average snow depth and snow density estimates. Even assuming shallow snow depths, including snow accumulation from this nearly 20×10^6 km^2 region will contribute to a larger Sturm et al. SWS estimate, increasing the difference from the global data sets considered here. The estimate based on Sturm et al. (1995) does make large assumptions by extrapolating representative snow depth and density values across large regions; nevertheless, it provides an observationally constrained data point for comparison.

Table 5
Estimated Snow Water Storage, in Cubic Kilometers, From Snow Cover Types From the Sturm et al. (1995) Snow Classification

Region	Area ($\times 10^6$ km^2)	Estimated average depth (m)	Estimated average density (g/cm^3)	Estimated snow water storage (km^3)
Tundra	16.6	0.3	0.4	1992
Taiga	11.4	0.5	0.3	1710
Maritime	3.6	2	0.3	2160

Using the new SMSM to identify regions with seasonally snow-covered mountains, we also show that the four data sets have similar fractions of SWS that accumulate in the snow-covered mountains, ranging from 23% to 30%. The global data products have more agreement in the mountains than overall, with all four within 23% of the mountain SWS average. For both global and mountain SWS, GLDAS differs the most from the four–data set mean, with 36% less global SWS than the average of 4,500 km^3 and 23% less SWS than the average of 1,108 km^3 for snow-covered mountains. We note that the SMSM and SWS time series only overlap over nine full water years, with the MOD10A2 analysis beginning in water year 2002 and the SWS analysis ending in water year 2010. However, we observe no substantial differences in long-term averages of SWS from MERRA-2 and ERA-Interim between 1980–2010 (the SWS time period used here) and 2002–2016 (the MOD10A2 time period used here; see Figure S5 and Table S6). Additional analysis for select MODIS granules comparing MOD10A2 over the full 2002–2016 MODIS period and the 2002–2010 overlap reveals that the seasonal snow classification is largely the same between the two periods (see Figure S8). Therefore, to maximize available MODIS observations, we based the SMSM on the full 2002–2016 period.

A consensus in SWS estimates, however, does not necessarily indicate the estimates are correct. We first compare ERA-Interim, GLDAS, and MERRA-2 to regional SWS estimates for CONUS and CONUS mountain ranges over a seven-year period, water years 2004 through 2010 (global VIC is unavailable for these years). For all four regions, the three global data sets produce the lowest estimates, with differences in maximum SWS up to 207 km^3 (−60%) and 135 km^3 (−50%) for CONUS when compared to VIC/Livneh and WRF/NCAR, respectively. By comparing over multiple years and multiple geographic regions, a pattern emerges that suggests the global data sets underestimate snow accumulation. This evaluation also demonstrates that SWS from WRF/NCAR is comparable to SNODAS, VIC/Livneh, and SNSR (for the Sierra Nevada). Further, though only available for one water year, WRF/Rep is also in agreement with the four regional data sets for the individual water years.

Though the regional data sets are available for multiple water years across CONUS, they do not include all of North America. To understand differences in SWS for all mountains of North America, we use the WRF/Rep data set. Comparing seasonally snow-covered mountain SWS from the four data sets to WRF/Rep in North America, there is an average underestimate of 602 km^3, which is similar to the amount of river runoff from the Mississippi River each year (Benke & Cushing, 2005). Assuming the North America SWS bias of 60% is similar across other continents, the global data products may be missing ~1,500 km^3 of global mountain SWS, increasing the four–data set average of mountain snow from ~1,100 km^3 to ~2,770 km^3. Missing 1,500 km^3 of water storage is on the order of over 2.5 years of Mississippi River runoff and about equal to 4% of the annual runoff from the world's rivers (National Research Council, 1991, Figure 2.6). Even if the mountain SWS bias in global data sets is only half or a third of what we see for North America, our results suggest that global models and reanalyses are likely biasing our understanding of the water budget due to underestimated SWS. We additionally note that this first calculation of "missing" SWS assumes that differences between WRF and the global data sets are similar across all mountain regions. The global data sets may have regionally different biases, varying not only from continent to continent, but also between mountain ranges. Until global WRF simulations are available, it is impossible to determine whether global data sets overestimate or underestimate snow simulated by WRF and to what magnitude. However, it is likely that the physical processes that are biased in North American mountains are also biased in global mountains. For example, early snowmelt biases may be attributed to warm temperature biases caused by coarse resolution and smoothed topography in global data sets, which would not be limited to North America. Therefore, while we cannot calculate SWS biases for the global mountains, we can assume that some processes are likely to behave similarly across mountain areas, allowing us to estimate biases based on North America evaluations.

The SWS underestimates we see in North America appear supported in other regions as well. We compare South American SWS from the four global data sets to values published by Cortés and Margulis (2017). In their reanalysis-based reconstruction of SWE for the extratropical Andes between 27°S and 37°S, Cortés and Margulis (2017) estimate a climatological average SWS of 27.7 km^3, more snow than three of the four data sets examined here have for the entire continent of South America. Using the new SMSM to extract mountain regions, no data set here has more than 10 km^3 of SWS for all mountains of South America, underestimating Cortés and Margulis (2017) by 64–96%.

The fraction of snow accumulation within the mountains also suggests a possible low SWS bias in the global data sets. Mountains are 23% of the global land area, but mountains in the four data products studied here have only 25% of global SWS, on average. VIC and MERRA-2 have the smallest percentage of SWS in the mountains (23%), and GLDAS has the largest (30%). Due to orographic effects and colder temperatures associated with high altitudes, mountains accumulate much deeper snowpacks than adjacent nonmountain lowland regions (Mudryk et al., 2015; Snauffer et al., 2016; Sturm et al., 1995). From previous work with WRF, the mountains of North America, which are 25% of the continental land area, hold a disproportionate 60% of the continental snow accumulation (Wrzesien et al., 2018). The four data products considered here only contain an average of 39% of North American SWS in the mountains. Of the four continents with sizable snow accumulation, only South American mountains have a disproportionate amount of snow (average 34%) relative to mountain area (18%). The small fractions of mountain SWS, as well as the regional multiproduct comparisons, suggest a bias in the representation of mountain snow accumulation in the four global data sets. Development of high-resolution data sets of SWS in seasonal mountain snow regions using RCMs (e.g., Wrzesien et al., 2018) and reanalyses-based satellite remote sensing (e.g., Cortés & Margulis, 2017; Margulis et al., 2016) would help to characterize both the extent of the mountain SWS underestimation and the reasons behind it.

Despite examples of global reanalyses underestimating SWS in mountain regions, there is little evidence to suggest similar biases in nonmountain lowland regions. Snauffer et al. (2016) compared gridded SWE to snow surveys in nonmountainous regions of British Columbia; they found the best performance in regions with lower elevation relief, with median bias ranging from −2 to −33 mm SWE (−2% to −37% the maximum monthly mean observed SWE), as compared to biases ranging from −266 to −579 mm (−32% to −69% the maximum monthly mean observed SWE) in the mountains. Similarly, Wrzesien, Durand, and Pavelsky (2019) noted that SWS biases in lowland regions (−8.8% to −22.7%) were much smaller than mountain biases (> −50%) for global data sets compared to WRF simulations. Estimating snow accumulation in lowland regions is also challenging, and since regions with lowland snow have a larger area than snow-covered mountains, a small average bias in lowland snow accumulation can lead to a large bias overall. Nevertheless, several studies (Snauffer et al., 2016; Wrzesien et al., 2018; Wrzesien, Durand, & Pavelsky, 2019) have now shown that global data products often have large underestimates in SWS in mountain regions, with smaller biases in lowlands.

5. Conclusion

Results presented here suggest that SWS biases in global data sets are likely hindering our understanding of the hydrologic cycle and our ability to produce reasonable representations of the water budget, expanding on results from other recent studies (Broxton et al., 2016; Henn et al., 2018; Wrzesien, Durand, & Pavelsky, 2019). Barring major advances in the remote sensing of snowpack (Bormann et al., 2018), regional models are likely the best option for improving spatiotemporal estimates of snow in mountain areas over large regions (Terzago et al., 2017). As we show here, global data products differ from regional model estimates of North American mountain SWS by a factor of 2, with potential global differences of ~1,500 km^3, on the order of more than 2 years of Mississippi River annual runoff. With millions of people relying on seasonal snow for water resources (Barnett et al., 2005) and with snowmelt being the main contributor to runoff for many rivers with mountain headwaters (Li et al., 2017), biases in snow accumulation will impact other aspects of the hydrologic cycle, such as runoff and soil moisture. These biases will reach beyond mountain areas, affecting assessment of water resources and hydrologic hazards for regions downstream.

Though the comparisons we show here suggest that global data sets are likely biased in their representations of seasonal snow accumulation, global models are often the only option for SWS estimates over large spatial scales. Regional models, though likely a better option for reasonable SWS simulations, are not available everywhere and have a high computational cost. Since representing snow accumulation on the mountain range scale remains the major challenge in snow hydrology (Bormann et al., 2018; Dozier et al., 2016), efforts are being made in the community to improve estimation of mountain snow accumulation, whether in single mountain ranges by combining modeling with remote sensing (Cortés & Margulis, 2017; Margulis et al., 2016) or over larger regions with RCMs (Liu et al., 2017; Wrzesien et al., 2018). Future work will continue

to improve and refine snow estimation through new modeling techniques, observational efforts, and the integration of models with observations.

Acknowledgments
This research was funded by NSF Innovations at the Nexus of Food Energy and Water Systems (INFEWS) grant CNS-1639268 (PI G. Characklis, UNC). GTOPO30 is available for download online (at https://lta.cr.usgs.gov/GTOPO30). GLDAS can be downloaded from the Goddard Earth Science Data and Information Services Center (GES DISC; disc.sci.gsfc.nasa.gov/hydrology/data-holdings). MERRA-2 may also be downloaded from the GES DISC. ERA-Interim can be accessed from the European Centre of Medium-Range Weather Forecasts (apps.ecmwf.int/datasets/data/interim-full-daily). VIC model output is available online (from hydro.washington.edu/SurfaceWaterGroup/Data/vic_global.html). The authors thank Daniel Viviroli and two anonymous reviewers for comments that improved the manuscript.

References

Bair, E. H., Rittger, K., Davis, R. E., Painter, T. H., & Dozier, J. (2016). Validating reconstruction of snow water equivalent in California's Sierra Nevada using measurements from the NASA Airborne Snow Observatory. *Water Resources Research*, *52*, 8437–8460. https://doi.org/10.1002/2016WR018704

Barnes, J. C., & Bowley, C. J. (1968). Snow cover distribution as mapped from satellite photography. *Water Resources Research*, *4*, 257–272. https://doi.org/10.1029/WR004i002p00257

Barnett, T. P., Adam, J. C., & Lettenmaier, D. P. (2005). Potential impacts of a warming climate on water availability in snow-dominated regions. *Nature*, *438*, 303–309. https://doi.org/10.1038/nature04141

Benke, A. C., & Cushing, C. E. (Eds) (2005). *Rivers of North America*. San Diego, CA: Elsevier/Academic Press.

Berg, N., & Hall, A. (2017). Anthropogenic warming impacts on California snowpack during drought. *Geophysical Research Letters*, *44*, 2511–2518. https://doi.org/10.1002/2016GL072104

Blyth, S., Groombridge, B., Lysenko, I., Miles, L., & Newton, A. C. (2002). *Mountain watch. Environmental change and sustainable development in mountains*. Cambridge: UNEP-WCMC.

Bormann, K. J., Brown, R. D., Derksen, C., & Painter, T. H. (2018). Estimating snow-cover trends from space. *Nature Climate Change*, *8*, 924–928. https://doi.org/10.1038/s41558-018-0318-3

Browne, T., Fox, R., & Funnell, D. (2004). The "invisible" mountains: Using GIS to examine the extent of mountain terrain in South Africa. *Mountain Research and Development*, *24*(1), 28–34. https://doi.org/10.1659/0276-4741(2004)024[0028:TIM]2.0.CO;2

Broxton, P. D., Zeng, X., & Dawson, N. (2016). Why do global reanalyses and land data assimilation products underestimate snow water equivalent? *Journal of Hydrometeorology*, *17*, 2743–2761. https://doi.org/10.1175/JHM-D-16-0056.1

Caldwell, P., Chin, H.-N. S., Bader, D. C., & Bala, G. (2009). Evaluation of a WRF dynamical downscaling simulation over California. *Climatic Change*, *95*(3-4), 499–521. https://doi.org/10.1007/s10584-009-9583-5

Carroll, T., Cline, D., Fall, G., Nilsson, A., Li, L., & Rost, A. (2001, April). NOHRSC operations and the simulation of snow cover properties for the coterminous US. In Proc. 69th Annual Meeting of the Western Snow Conf (pp. 1-14).

Chen, M., Shi, W., Xie, P., Silva, V. B. S., Kousky, V. E., Wayne Higgins, R., & Janowiak, J. E. (2008). Assessing objective techniques for gauge-based analyses of global daily precipitation. *Journal of Geophysical Research*, *113*, D04110. https://doi.org/10.1029/2007JD009132

Clow, D. W., Nanus, L., Verdin, K. L., & Schmidt, J. (2012). Evaluation of SNODAS snow depth and snow water equivalent estimates for the Colorado Rocky Mountains, USA. *Hydrological Processes*, *26*(17), 2583–2591. https://doi.org/10.1002/hyp.9385

Cortés, G., & Margulis, S. (2017). Impacts of El Niño and La Niña on interannual snow accumulation in the Andes: Results from a high-resolution 31 year reanalysis. *Geophysical Research Letters*, *44*, 6859–6867. https://doi.org/10.1002/2017GL073826

Dee, D. P., Uppala, S. M., Simmons, A. J., Berrisford, P., Poli, P., Kobayashi, S., et al. (2011). The ERA-Interim reanalysis: Configuration and performance of the data assimilation system. *Quarterly Journal of the Royal Meteorological Society*, *137*(656), 553–597. https://doi.org/10.1002/qj.828

Dozier, J., Bair, E. H., & Davis, R. E. (2016). Estimating the spatial distribution of snow water equivalent in the world's mountains. *Wiley Interdisciplinary Reviews Water*, *3*(3), 461–474. https://doi.org/10.1002/wat2.1140

Etchevers, P., Martin, E., Brown, R., Fierz, C., Lejeune, Y., Bazile, E., et al. (2004). Validation of the energy budget of an alpine snowpack simulated by several snow models (SnowMIP project). *Annals of Glaciology*, *38*, 150–158. https://doi.org/10.3189/172756404781814825

Hall, D. K., & Riggs, G. A. (2016). MODIS/Aqua Snow Cover 8-Day L3 Global 500 m grid, Version 6. Boulder, Colorado USA. NASA National Snow and Ice Data Center Distributed Active Archive Center. https://doi.org/10.5067/MODIS/MYD10A2.006. [April 2018].

Hall, D. K., Riggs, G. A., Salomonson, V. V., DiGirolamo, N. E., & Bayr, K. J. (2002). MODIS snow-cover products. *Remote Sensing of Environment*, *83*(1–2), 181–194. https://doi.org/10.1016/S0034-4257(02)00095-0

Hedrick, A., Marshall, H. P., Winstral, A., Elder, K., Yueh, S., & Cline, D. (2015). Independent evaluation of the SNODAS snow depth product using regional-scale lidar derived measurements. *The Cryosphere*, *9*(1), 13–23. https://doi.org/10.5194/tc-9-13-2015 Henn, B., Newman, A. J., Livneh, B., Daly, C., & Lundquist, J. D. (2018). An assessment of differences in gridded precipitation datasets in complex terrain. *Journal of Hydrology*, *556*, 1205–1219. https://doi.org/10.1016/j.jhydrol.2017.03.008

Huddleston, B., Ataman, E., & d'Ostiani, L. F. (2003). *Towards a GIS based analysis of mountain environment and population* (p. 26). Rome: FAO.

Jin, J., & Wen, L. (2012). Evaluation of snowmelt simulation in the Weather Research and Forecasting model. *Journal of Geophysical Research*, *117*(D10), D10110. https://doi.org/10.1029/2011JD016980

Justice, C. O., Vermote, E., Townshend, J. R. G., Defries, R., Roy, D. P., Hall, D. K., et al. (1998). The Moderate Resolution Imaging Spectroradiometer (MODIS): Land remote sensing for global change research. *Geoscience and Remote Sensing, IEEE Transactions on*, *36*(4), 1228–1249. https://doi.org/10.1109/36.701075

Kapos, V., Rhind, J., Edwards, M., Price, M. F., & Ravilious, C. (2000). Developing a map of the world's mountain forests. In M. F. Price, & N. Butt (Eds.), *Forests in sustainable mountain development: A state-of-knowledge report for 2000*, (pp. 4–9). Wallingford: CAB International.

Körner, C., Jetz, W., Paulsen, J., Payne, D., Rudmann-Maurer, K., & Spehn, E. M. (2017). A global inventory of mountains for bio-geographical applications. *Alpine Botany*, *127*(1), 1–15. https://doi.org/10.1007/s00035-016-0182-6

Körner, C., Paulsen, J., & Spehn, E. M. (2011). A definition of mountains and their bioclimatic belts for global comparisons of biodiversity data. *Alpine Botany*, *121*, 73–78. https://doi.org/10.1007/s00035-011-0094-4

Lettenmaier, D. P., Alsdorf, D., Dozier, J., Huffman, G. J., Pan, M., & Wood, E. F. (2015). Inroads of remote sensing into hydrologic science during the WRR era. *Water Resources Research*, *51*, 7309–7342. https://doi.org/10.1002/2015WR017616

Li, D., Wrzesien, M. L., Durand, M., Adam, J., & Lettenmaier, D. P. (2017). How much runoff originates as snow in the western United States, and how will that change in the future? *Geophysical Research Letters*, *44*, 6163–6172. https://doi.org/10.1002/2017GL073551

Liang, X., Lettenmaier, D. P., Wood, E. F., & Burges, S. J. (1994). A simple hydrologically based model of land surface water and energy fluxes for general circulation models. *Journal of Geophysical Research*, *99*, 14,415–14,428. https://doi.org/10.1029/94JD00483

Liu, C., Ikeda, K., Rasmussen, R., Barlage, M., Newman, A. J., Prein, A. F., et al. (2017). Continental-scale convection-permitting modeling of the current and future climate of North America. *Climate Dynamics*, *49*(1-2), 71–95. https://doi.org/10.1007/s00382-016-3327-9

Livneh, B., Rosenberg, E. A., Lin, C., Nijssen, B., Mishra, V., Andreadis, K. M., et al. (2013). A long-term hydrologically based dataset of land surface fluxes and states for the conterminous United States: Update and extensions. *Journal of Climate*, *26*(23), 9384–9392. https://doi.org/10.1175/JCLI-D-12-00508.1

Margulis, S. A., Cortés, G., Girotto, M., & Durand, M. (2016). A Landsat-era Sierra Nevada snow reanalysis (1985–2015). *Journal of Hydrometeorology*, *17*(4), 1203–1221. https://doi.org/10.1175/JHM-D-15-0177.1

Messerli, B., & Ives, J. D. (Eds) (1997). *Mountains of the world: A global priority*. New York and Carnforth: Parthenon Publishing.

Meybeck, M., Green, P., & Vörösmarty, C. (2001). A new typology for mountains and other relief classes: An application to global continental water resources and population distribution. *Mountain Research and Development*, *21*(1), 34–45. https://doi.org/10.1659/0276-4741(2001)021[0034:ANTFMA]2.0.CO;2

Minder, J. R., Letcher, T. W., & Skiles, S. M. K. (2016). An evaluation of high-resolution regional climate model simulations of snow cover and albedo over the Rocky Mountains, with implications for the simulated snow-albedo feedback. *Journal of Geophysical Research: Atmospheres*, *121*, 9069–9088. https://doi.org/10.1002/2016JD024995

Minder, J. R., Mote, P. W., & Lundquist, J. D. (2010). Surface temperature lapse rates over complex terrain: Lessons from the Cascade Mountains. *Journal of Geophysical Research*, *115*, D14122. https://doi.org/10.1029/2009JD013493

Mudryk, L. R., Derksen, C., Kushner, P. J., & Brown, R. (2015). Characterization of Northern Hemisphere snow water equivalent datasets, 1981–2010. *Journal of Climate*, *28*, 8037–8051. https://doi.org/10.1175/JCLI-D-15-0229.1

Musselman, K. N., Clark, M. P., Liu, C., Ikeda, K., & Rasmussen, R. (2017). Slower snowmelt in a warmer world. *Nature Climate Change*, *7*(3), 214. https://doi.org/10.1038/nclimate3225

Musselman, K. N., Lehner, F., Ikeda, K., Clark, M. P., Prein, A. F., Liu, C., et al. (2018). Projected increases and shifts in rain-on-snow flood risk over western North America. *Nature Climate Change*, *8*(9), 808–812. https://doi.org/10.1038/s41558-018-0236-4

National Research Council (1991). *Opportunities in the hydrologic sciences*. Washington, D.C: National Academies Press. https://doi.org/10.17226/1543

Nijssen, B., O'Donnell, G., Lettenmaier, D. P., Lohmann, D., & Wood, E. F. (2001). Predicting the discharge of global rivers. *Journal of Climate*, *14*(15), 3307–3323. https://doi.org/10.1175/1520-0442(2001)014<3307:PTDOGR>2.0.CO;2

Nijssen, B., O'Donnell, G. M., Hamlet, A. F., & Lettenmaier, D. P. (2001). Hydrologic sensitivity of global rivers to climate change. *Climatic Change*, *50*(1-2), 143–175. https://doi.org/10.1023/A:1010616428763

Nijssen, B., Schnur, R., & Lettenmaier, D. P. (2001). Global retrospective estimation of soil moisture using the Variable Infiltration Capacity land surface model, 1980-93. *Journal of Climate*, *14*(8), 1790–1808. https://doi.org/10.1175/1520-0442(2001)014<1790:GREOSM>2.0.CO;2

Niu, G. Y., Yang, Z. L., Mitchell, K. E., Chen, F., Ek, M. B., Barlage, M., et al. (2011). The community Noah land surface model with multiparameterization options (Noah-MP): 1. Model description and evaluation with local-scale measurements. *Journal of Geophysical Research*, *116*, D12109. https://doi.org/10.1029/2010JD015139

Nolin, A. W. (2010). Recent advances in remote sensing of seasonal snow. *Journal of Glaciology*, *56*, 1141–1150. https://doi.org/10.3189/002214311796406077

Painter, T. H., Berisford, D. F., Boardman, J. W., Bormann, K. J., Deems, J. S., Gehrke, F., et al. (2016). The Airborne Snow Observatory: Fusion of scanning lidar, imaging spectrometer, and physically-based modeling for mapping snow water equivalent and snow albedo. *Remote Sensing of Environment*, *184*, 139–152. https://doi.org/10.1016/j.rse.2016.06.018

Painter, T. H., Bryant, A. C., & Skiles, S. M. (2012). Radiative forcing by light absorbing impurities in snow from MODIS surface reflectance data. *Geophysical Research Letters*, *39*, L17502. https://doi.org/10.1029/2012GL052457

Painter, T. H., Rittger, K., McKenzie, C., Slaughter, P., Davis, R. E., & Dozier, J. (2009). Retrieval of subpixel snow-covered area, grain size, and albedo from MODIS. *Remote Sensing of Environment*, *113*, 868–879. https://doi.org/10.1016/j.rse.2009.01.001

Pavelsky, T. M., Kapnick, S., & Hall, A. (2011). Accumulation and melt dynamics of snowpack from a multiresolution regional climate model in the central Sierra Nevada, California. *Journal of Geophysical Research*, *116*, D16115. https://doi.org/10.1029/2010JD015479

Petersky, R., & Harpold, A. (2018). Now you see it, now you don't: A case study of ephemeral snowpacks and soil moisture response in the Great Basin, USA. *Hydrology and Earth System Sciences*, *22*(9), 4891–4906. https://doi.org/10.5194/hess-22-4891-2018

Pfeffer, W. T., Arendt, A. A., Bliss, A., Bolch, T., Cogley, J. G., Gardner, A. S., et al., & The Randolph Consortium (2014). The Randolph Glacier Inventory: A globally complete inventory of glaciers. *Journal of Glaciology*, *60*(221), 537–552. http://doi.org/10.3189/2014JoG13J176

Platts, P. J., Burgess, N. D., Gereau, R. E., Lovett, J. C., Marshall, A. R., McCLEAN, C. J., et al. (2011). Delimiting tropical mountain ecoregions for conservation. *Environmental Conservation*, *38*(3), 312–324. https://doi.org/10.1017/S0376892911000191

Prein, A. F., Rasmussen, R. M., Ikeda, K., Liu, C., Clark, M. P., & Holland, G. J. (2017). The future intensification of hourly precipitation extremes. *Nature Climate Change*, *7*(1), 48. https://www.nature.com/articles/nclimate3168

Qian, Y., Ghan, S. J., & Leung, L. R. (2010). Downscaling hydroclimatic changes over the western US based on CAM subgrid scheme and WRF regional climate simulations. *International Journal of Climatology*, *30*(5), 675–693. https://doi.org/10.1002/joc.1928

Rasmussen, R., and C. Liu (2017), High resolution WRF simulations of the current and future climate of North America, https://doi.org/10.5065/D6V40SXP, Research Data Archive at the National Center for Atmospheric Research, Computational and Information Systems Laboratory, Boulder, Colo. Accessed 11 Jun 2019.

Rasmussen, R., Liu, C., Ikeda, K., Gochis, D., Yates, D., Chen, F., et al. (2011). High-resolution coupled climate runoff simulations of seasonal snowfall over Colorado: A process study of current and warmer climate. *Journal of Climate*, *24*(12), 3015–3048. https://doi.org/10.1175/2010JCLI3985.1

Raup, B., Racoviteanu, A., Khalsa, S. J. S., Helm, C., Armstrong, R., & Arnaud, Y. (2007). The GLIMS geospatial glacier database: A new tool for studying glacier change. *Global and Planetary Change*, *56*(1-2), 101–110. https://doi.org/10.1016/j.gloplacha.2006.07.018

RGI Consortium (2017). Randolph Glacier Inventory—A dataset of global glacier outlines: Version 6.0: Technical report, Global Land Ice Measurements from Space, Colorado, USA. Digital Media. DOI: https://doi.org/10.7265/N5-RGI-60

Rienecker, M. M., Suarez, M. J., Gelaro, R., Todling, R., Bacmeister, J., Liu, E., et al. (2011). MERRA: NASA's Modern-Era Retrospective Analysis for Research and Applications. *Journal of Climate*, *24*(14), 3624–3648. https://doi.org/10.1175/JCLI-D-11-00015.1

Rodell, M., Houser, P. R., Jambor, U., Gottschalck, J., Mitchell, K., Meng, C. J., et al. (2004). The Global Land Data Assimilation System. *Bulletin of the American Meteorological Society*, *85*(3), 381–394. https://doi.org/10.1175/BAMS-85-3-381

Sheffield, J., Goteti, G., & Wood, E. F. (2006). Development of a 50-year high-resolution global dataset of meteorological forcings for land surface modeling. *Journal of Climate*, *19*, 3088–3111. https://doi.org/10.1175/JCLI3790.1

Skofronick-Jackson, G. M., Johnson, B. T., & Munchak, S. J. (2013). Detection thresholds of falling snow from satellite-borne active and passive sensors. *IEEE Transactions on Geoscience and Remote Sensing*, *51*(7), 4177–4189. https://doi.org/10.1109/TGRS.2012.2227763

Snauffer, A. M., Hsieh, W. W., & Cannon, A. J. (2016). Comparison of gridded snow water equivalent products with in situ measurements in British Columbia, Canada. *Journal of Hydrology*, *541*, 714–726. https://doi.org/10.1016/j.jhydrol.2016.07.027

Sturm, M., Goldstein, M. A., & Parr, C. (2017). Water and life from snow: A trillion dollar science question. *Water Resources Research*, *53*, 3534–3544. https://doi.org/10.1002/2017WR020840

Sturm, M., Holmgren, J., & Liston, G. E. (1995). A seasonal snow cover classification system for local to global applications. *Journal of Climate*, *8*(5), 1261–1283. https://doi.org/10.1175/1520-0442(1995)008<1261:ASSCCS>2.0.CO;2

Syed, T. H., Famiglietti, J. S., & Chambers, D. P. (2009). GRACE-based estimates of terrestrial freshwater discharge from basin to continental scales. *Journal of Hydrometeorology*, *10*(1), 22–40. https://doi.org/10.1175/2008JHM993.1

Syed, T. H., Famiglietti, J. S., Chambers, D. P., Willis, J. K., & Hilburn, K. (2010). Satellite-based global-ocean mass balance estimates of interannual variability and emerging trends in continental freshwater discharge. *Proceedings of the National Academy of Sciences*, *107*(42), 17,916–17,921. https://doi.org/10.1073/pnas.1003292107

Takala, M., Luojus, K., Pulliainen, J., Derksen, C., Lemmetyinen, J., Kärnä, J. P., et al. (2011). Estimating Northern Hemisphere snow water equivalent for climate research through assimilation of space-borne radiometer data and ground-based measurements. *Remote Sensing of Environment*, *115*(12), 3517–3529. https://doi.org/10.1016/j.rse.2011.08.014

Tapley, B. D., Bettadpur, S., Ries, J. C., Thompson, P. F., & Watkins, M. M. (2004). GRACE measurements of mass variability in the Earth system. *Science*, *305*(5683), 503–505. https://doi.org/10.1126/science.1099192

Terzago, S., von Hardenberg, J., Palazzi, E., & Provenzale, A. (2014). Snowpack changes in the Hindu Kush–Karakoram–Himalaya from CMIP5 global climate models. *Journal of Hydrometeorology*, *15*(6), 2293–2313. https://doi.org/10.1175/JHM-D-13-0196.1

Terzago, S., von Hardenberg, J., Palazzi, E., & Provenzale, A. (2017). Snow water equivalent in the Alps as seen by gridded data sets, CMIP5 and CORDEX climate models. *The Cryosphere*, *11*(4), 1625–1645. https://doi.org/10.5194/tc-11-1625-2017

Thompson, G., Field, P. R., Rasmussen, R. M., & Hall, W. D. (2008). Explicit forecasts of winter precipitation using an improved bulk microphysics scheme. Part II: Implementation of a new snow parameterization. *Monthly Weather Review*, *136*(12), 5095–5115. https://doi.org/10.1175/2008MWR2387.1

Viviroli, D., Dürr, H. H., Messerli, B., Meybeck, M., & Weingartner, R. (2007). Mountains of the world, water towers for humanity: Typology, mapping, and global significance. *Water Resources Research*, *43*, W07447. https://doi.org/10.1029/2006WR005653

Viviroli, D., & Weingartner, R. (2004). The hydrological significance of mountains: From regional to global scale. *Hydrology and Earth System Sciences*, *8*(6), 1016–1029. https://doi.org/10.5194/hess-8-1017-2004

Wahr, J., Swenson, S., Zlotnicki, V., & Velicogna, I. (2004). Time-variable gravity from GRACE: First results. *Geophysical Research Letters*, *31*, L11501. https://doi.org/10.1029/2004GL019779

Waliser, D., Kim, J., Xue, Y., Chao, Y., Eldering, A., Fovell, R., et al. (2011). Simulating cold season snowpack: The impact of snow albedo and multi-layer snow physics. *Climatic Change*, *109*(S1), 95–117. https://doi.org/10.1007/s10584-011-0312-5

Wrzesien, M., & Durand, M. (2018). *Weather Research and Forecasting (WRF) North American Mountain Snow Data, Version 1*. Boulder, Colorado USA: NSIDC: National Snow and Ice Data Center. https://doi.org/10.5067/W4JHZBCRCNLX

Wrzesien, M. L., Durand, M. T., & Pavelsky, T. M. (2019). A reassessment of North American river basin cool-season precipitation: Developments from a new mountain climatology data set. *Water Resources Research*, *55*, 3502–3519. https://doi.org/10.1029/2018WR024106

Wrzesien, M. L., Durand, M. T., Pavelsky, T. M., Howat, I. M., Margulis, S. A., & Huning, L. S. (2017). Comparison of methods to estimate snow water equivalent at the mountain range scale: A case study of the California Sierra Nevada. *Journal of Hydrometeorology*, *18*, 1101–1119. https://doi.org/10.1175/JHM-D-16-0246.1

Wrzesien, M. L., Durand, M. T., Pavelsky, T. M., Kapnick, S. B., Zhang, Y., Guo, J., & Shum, C. K. (2018). A new estimate of North American mountain snow accumulation from regional climate model simulations. *Geophysical Research Letters*, *45*, 1423–1432. https://doi.org/10.1002/2017GL076664

Wrzesien, M. L., Pavelsky, T. M., Durand, M. T., Dozier, J., & Lundquist, J. D. (2019). Global Seasonal Mountain Snow Mask from MODIS MOD10A2. Zenodo. http://doi.org/10.5281/zenodo.2626737

Wrzesien, M. L., Pavelsky, T. M., Kapnick, S. B., Durand, M. T., & Painter, T. H. (2015). Evaluation of snow cover fraction for regional climate simulations in the Sierra Nevada. *International Journal of Climatology*, *35*(9), 2472–2484. https://doi.org/10.1002/joc.4136

Xie, P., & Arkin, P. A. (1997). Global precipitation: A 17-year monthly analysis based on gauge observations, satellite estimates, and numerical model outputs. *Bulletin of the American Meteorological Society*, *78*(11), 2539–2558. https://doi.org/10.1175/1520-0477(1997)078,2539:GPAYMA.2.0.CO;2

Xie, P., Chen, M., Yang, S., Yatagai, A., Hayasaka, T., Fukushima, Y., & Liu, C. (2007). A gauge-based analysis of daily precipitation over East Asia. *Journal of Hydrometeorology*, *8*(3), 607–626. https://doi.org/10.1175/JHM583.1

Zhou, T., Nijssen, B., Gao, H., & Lettenmaier, D. P. (2016). The contribution of reservoirs to global land surface water storage variations. *Journal of Hydrometeorology*, *17*, 309–325. https://doi.org/10.1175/jhm-d-15-0002.1